12th AIAA Aviation Technology, Integration, and Operations (ATIO) Conference and 14th AIAA/ISSM
17 - 19 September 2012, Indianapolis, Indiana

AIAA 2012-5402

Aerodynamic Design Considerations and Shape Optimization of Flying Wings in Transonic Flight

M. Zhang[1], A. Rizzi[1], P. Meng[1], R. Nangia[2], R. Amiree[3] and O. Amoignon[3]
[1]*Royal Institute of Technology (KTH), 10044 Stockholm, Sweden*
[2]*Nangia Aero Research Associates, Bristol BS8 1QU, UK*
[3]*Swedish Defence Research Agency (FOI), 16490 Stockholm, Sweden*

This paper provides a technique that minimize the cruise drag (or maximize L/D) for a blended wing body transport with a number of constraints. The wing shape design is done by splitting the problem into 2D airfoil design and 3D twist optimization with a frozen planform. A 45% to 50% reduction of inviscid drag is finally obtained, with desired pitching moment. The results indicate that further improvement can be obtained by modifying the planform and varying the camber more aggressively.

I. Introduction & Overview

Historically, the flying wing aircraft concept dates as far back as to 1910, when Hugo Junkers believed the flying wing's potentially large internal volume and low drag made it capable of carrying a reasonable amount of payload efficiently over a large distance. In the 30's and 40's the flying wing concept was studied extensively and a series of designs were tried out, with the Horten Ho 229 fighter being the most famous one (Fig 1). Currently, a Blended Wing Body configuration is being investigated by NASA and its industry partners, which incorporates both a flying wing and and the features of conventional transport aircraft (Fig 2). The BWB is quiet, strong, inexpensive to build, and because of its economical performance is a promising candidate for the future large airliner. Estimates indicate that it is capable of carrying larger payload with better fuel efficiency, for both civilian and military applications, than conventional configurations.

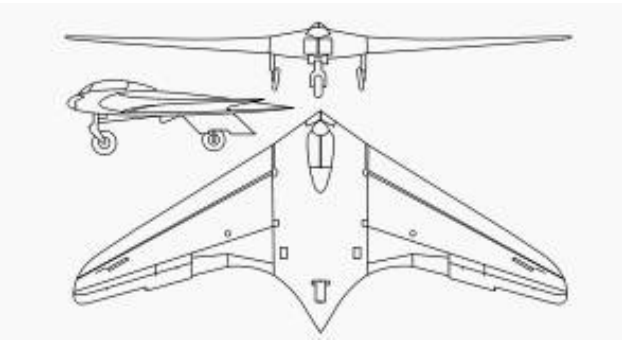

Figure 1. Horten Ho 229[1]

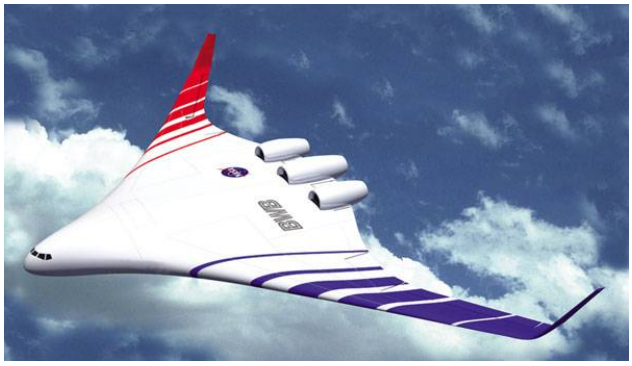

Figure 2. Blended Wing Body[2]

The BWB aircraft eliminates the tail of the conventional aircraft and blends the fuselage with the wing. Essentially a flying wing, it has been studied extensively by Liebeck *et al.*[17] and many others. The BWB center-body provides lift which improves the aerodynamic performance by reducing the wing loading, compared to the cylindrical fuselage of a conventional aircraft. Moreover, because of its smaller outer wing, the decrease in wetted area relative to a similar sized conventional aircraft translates into an increased lift-to-drag ratio. For a very large BWB the low wetted-area-to-volume ratio compounds the benefit.

The paper presents an optimization technique applied to the transonic-wing design of the *MOB* BWB aircraft studied by Ciampa *et al.*[3]

A good deal of the aerodynamic design work has been carried out with Euler-based optimization techniques and the results have demonstrated the potential for 'discovering' aerodynamically efficient features of flying wings. Using higher-fidelity optimization at the *conceptual* design phase may lead the way to new and innovative shapes that might not have been discovered otherwise. Typical components in the tool-chest used to explore the conceptual design space are: a CFD flow solver, gradient-evaluation algorithm and optimizer, and an integrated geometry and mesh manager which provides a flexible parametrization linked with a robust and rapid mesh movement algorithm.

We focus on the transonic-cruise design with an Euler solver and gradient-based optimization to determine the minimum wave-drag and induced-drag design. The baseline configuration is the zero-twist and zero-camber version of the Ciampa *et al.*[3] geometry. As constraints, the planform and airfoil thickness at each section are held to the baseline values. Other constraints are formulated as needed, such as limits on pitching moment, etc. The optimization problem then is to find the spanwise wing-twist distribution and the camber of each airfoil section. Key considerations include: wave drag, spanwise load distribution, aerofoil section design, and 3D shaping of the wing for performance improvement.

A. Challenges to Design Highly Swept Flying Wing

Highly swept wings, always accompanied with low aspect ratio or highly taper ratio, will cause the leading-edge suction peaks to stall at at some critical lift coefficient, and the lift-induced drag increases accordingly. The other challenge is that the outer wing, with increasing sweep angle and decreasing taper ratio, is highly loaded. It means that the tip is prone to stall first, which causes a series of problems. First of all, the ailerons would lose their effectiveness. Since the tip stall will cause a local lift loss, the large sweep would shift the aerodynamic center forward and cause a nose-up pitching moment. In this state the flying wing is difficult to control. If the platform is frozen, the designer is induced to increase the outboard *washout* to release tip loads.

Our specific goal here is to explore the conceptual design space of the BWB to see if equal or superior aerodynamic performance can be achieved compared to a conventional large commercial transport, e.g. the B-777, or A-380. Typically the aspect ratio of the BWB is lower, e.g. around 5, compared to approximately 8 to 10 for current civil airliners. Figure 3 shows that the tip-stall tendencies increase with sweepback angle. The MOB BWB studied in this paper and the Boeing blended-wing-body X-48 lie on the central part, and have planforms more similar in fact to the F-18 than to the B-777.

For low-speed climb-out substantial lift, around $C_L = 0.6$, is required at a limited range of angle of attack because of passenger deck-angle limitations. The BWB advantage is the promise of lower drag, and the challenge, as well as the opportunity, occurs at the transonic cruise condition, say around $M_{cr} = 0.8$. Interference drag is reduced due to the elimination and reduction of junctions between the wings and the fuselage, resulting in a more streamlined shape for the BWB. The naturally area-ruled shape of the BWB means that higher cruise Mach numbers ought to be more easily attainable without changes in the basic configuration geometry. In fact, the BWB's cross-sectional area variation resembles that of the body of minimum wave drag due to volume (Sears-Haack body) and thus has favorable transonic wave drag.

Certain aerodynamic challenges also exist along side the promises of the BWB to deliver lower drag, especially at transonic cruise. For instance, in order to accommodate passengers, cargo and landing gear, the BWB requires inboard airfoils of unusually large thickness-to-chord ratio, (e.g. 17% thick), which must also be maintained along a considerable portion of the chord length, making it a very challenging design problem to maintain low wave drag. This inboard geometry may also impact unusually strong shock wave build-up on the outer wing.

II. Design Procedures and Algorithm

The power of aerodynamic shape optimization (ASO) based on Computational Fluid Dynamics (CFD) is to automatically improve the design of aircraft components. Today, the fastest approach in this type of optimization is a combination of gradient algorithms for non linear constrained optimization, such as Sequential Quadratic Programming, with a solver of the adjoint flow equations. The unstructured flow solver Edge[9] solves the compressible Euler equations and its adjoint.[10] These must be integrated efficiently

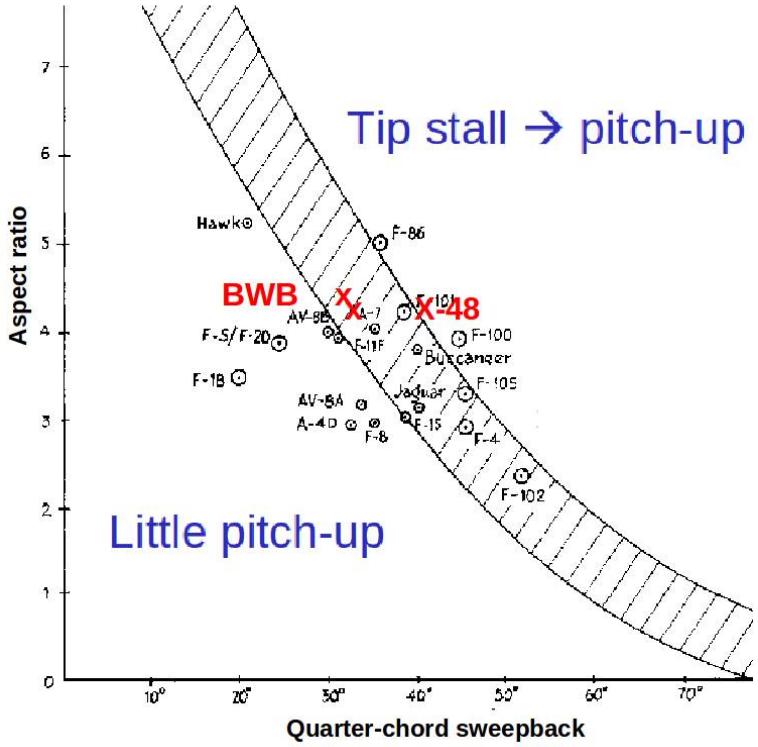

Figure 3. Planform effect on tip stalling leading to pitch-up (re-produced from Whitford,[27] Fig. 41

with the geometrical parametrization and mesh adaption by deformation, as explained by Amoignon.[12] The formal optimization problem that will be solved then aims at the reduction of the inviscid drag, i.e. wave drag due to shocks and lift-induced drag, at one design point defined by the Mach number M and angle-of-attack α, or lift coefficient, including constraints on the lift, pitching moment and geometrical characteristics like thicknesses and wing planform. Such an optimal design problem takes the form:

$$\begin{cases} \min\limits_{\boldsymbol{a}\in\mathbb{R}^n} C_D\left(\mathbf{w},\mathbf{X}\right) \quad \text{subject to} \\ \qquad C_L\left(\mathbf{w},\mathbf{X}\right) \geq l_0\,, \\ l_1 \leq C_m\left(\mathbf{w},\mathbf{X}\right) \leq l_2\,, \\ \qquad g_j\left(\mathbf{X_\Gamma}\right) \leq 0\,, 1 \leq j \leq m\,, \\ \mathbf{R}\left(\mathbf{w}_k,\mathbf{X},M,\alpha\right) = \mathbf{0}\,, \\ \qquad \mathbf{M}\left(\mathbf{X},\mathbf{X}_\Gamma\right) = \mathbf{0}\,, \\ \qquad \mathbf{S}\left(\mathbf{X}_\Gamma,\mathbf{a}\right) = \mathbf{0}\,, \end{cases} \tag{1}$$

where $\boldsymbol{a}$ is the vector of parameters being optimized, the aerodynamic coefficients C_D, C_L and C_m denote the drag, the lift and pitching moment coefficients, l_0, l_1 and l_2 are real numbers and g_j denotes the j^{th} geometrical constraint. For application in this paper the design point will be transonic cruise at $M_{cr} = 0.8$ and $C_L = 0.3$. The discretized flow equations, mesh adaption equation and parametrization, respectively, are described above as systems of equations written in residual form $\mathbf{R}$, $\mathbf{M}$ and $\mathbf{S}$ in order to have as light notations as possible. The vector of mesh coordinates is $\mathbf{X}$, its restriction on the shape being deformed denoted $\mathbf{X}_\Gamma$, and the vector of all flow unknowns (density, velocity and pressure) at all nodes in the mesh $\mathbf{w}$. The adjoint of the discretized flow equations, the mesh deformation, and the details of the gradient computation are presented in detail by Amoignon and Berggren.[11]

The mesh-deformation - adjoint scheme introduced above guarantees smoothness of objective function with parameter variation, and is certainly much to be recommended. The current paper has instead used the

loose coupling of CFD solver with CAD and mesh software, so our focus here will be on the integration of the CAD parametrization in the optimization loop using the surface modeler-mesher sumo[7] which constructs the mesh on the parametric surface patches by a 3D circumsphere criterion to produce a 3D-Delaunay grid. One may then worry about differentiability, but that has not created any noticeable problems in the computations reported.

A. Engineer-in-Loop: Re-meshing Technique

In this paper we choose re-meshing together with a finite-difference approximation of gradients and involve the engineer very much in the loop. Optimization steps are used as indications to the engineer on what direction her design modifications should choose. Figure 4 shows the flow chart of solving the optimization problem. The geometry is parameterized and sent to CAD and the mesh generator sumo, CFD computations are carried out on a

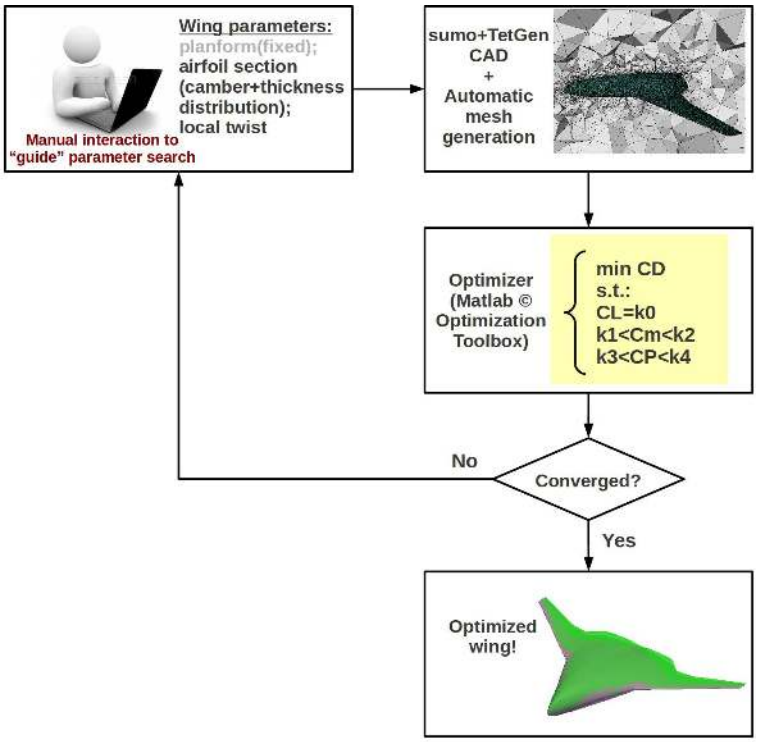

Figure 4. Flow chart of the optimization procedure with the engineer in the loop to guide the search

cluster and the results are sent back to the optimizer. The optimizer assesses progress towards a minimum. The iterations will stop once the optimizer estimates that future improvements will be small, e.g. by assessing gradients. As explained below, it is a two-step procedure, and a distinguishing feature of our approach is that the engineer is very much in the loop to guide the parameter search.

The Matlab©Optimization Toolbox provides a number of algorithms. In this paper an *interior-point* algorithm[18] is used. In order to capture the difference in geometry when small variations of geometrical parameters are applied, the minimum difference change to all the design parameters (to calculate the Jacobian) is restricted to a relatively large number 0.01. To reduce the computation time, the gradient is calculated by finite differences of the function using parallel computing: all derivatives are computed at once, each one on its own pc cluster node.

B. sumo-Based Wing Geometry: Parametrization & Re-Meshing

The surface modeler sumo defines the wing surface by a given number of airfoils specified along the span of the wing (Fig 5).

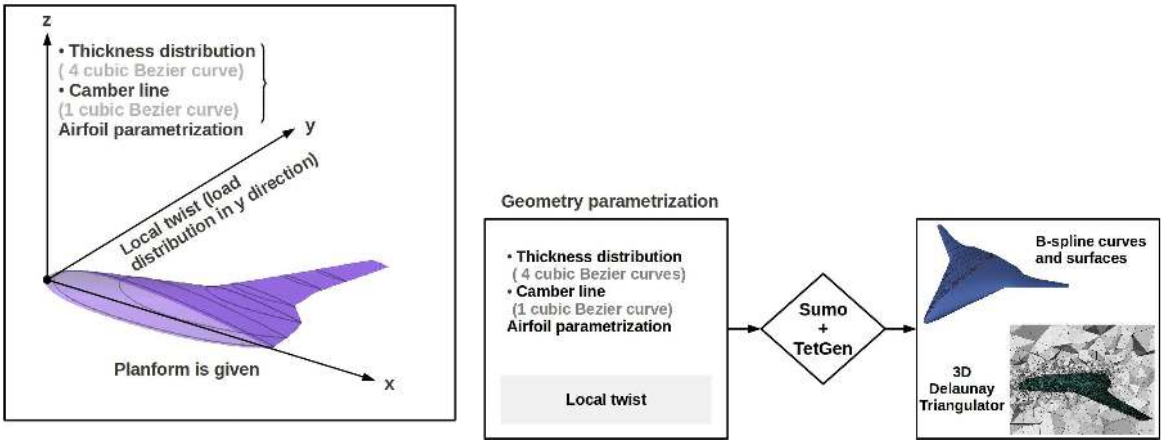

(a) Creating wing surface with sumo

(b) sumo-based geometry parametrization

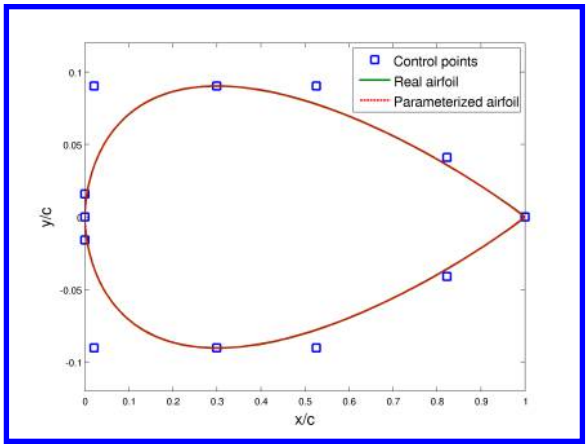

(c) Symmetric airfoil parametrization by four cubic Bezier curves

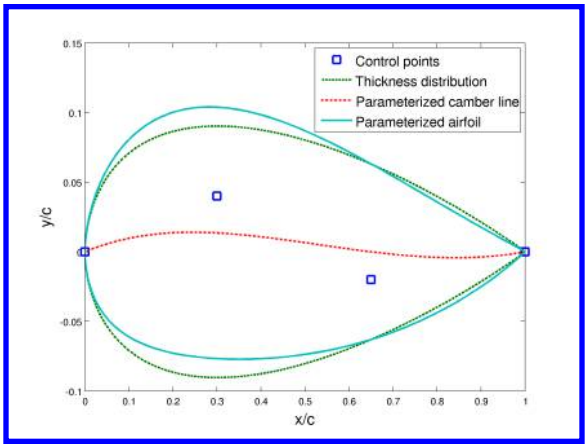

(d) Cambered airfoil parametrization by adding the thickness distribution to a parameterized camber line (a cubic Bezier curve) controlled by four control points

Figure 5. Airfoil-wing parametrization and re-meshing: a two-step procedure.

It stores the cross-sectional information (points) as skeletons for the components e.g., wings, fuselages, nacelles, and pylons. All the surfaces are represented by bi-parametric patches of the form $(x, y, z) = S(u, v)$, where at least the first derivatives with respect to the parameters u and v are continuous[7] across patch boundaries and the parametrization is such that G1-continuity ensues.. It provides an easy-to-change environment to modify/re-construct the geometry by specifying the global or/and local leading edge positions, cross-section points, twists, rotations, etc., which are the parameters we control.

sumo together with the TetGen[28] automatic tetrahedral mesher can provide a high-quality unstructured volume mesh for Euler computation in few seconds.

To proceed step by step with a reduced number of design parameters at each step, the overall optimization task is split into sequential processes, 2D airfoil design and 3D twist optimization. which again choice of thickness distribution and choice of camber, The 2D level is again split into two, with airfoil geometry treated as a combination of thickness distribution and the added camber effect. The overall problem is not exactly separable in this way, so there is no guarantee of finding the overall optimum in this way, but we have found the decomposition very instructive for the engineer. Anyway, there is no guarantee of finding global optima, so we are content to obtain improvements and to understand why the proposed change was beneficial.

- the thickness distribution is obtained from a parameterized symmetric airfoil, similarly to Venkataraman.[19] Four control points, or seven design variables are used for each section. There are six independent sections to make the wing, thus 42 design variables to be optimized at this stage;

- the camber line of each section is parameterized by a cubic Bezier curve, with two control points sitting in the nose and the tail and two free for a total of 4 dof per section. The cambered airfoil is obtained by adding the thickness distribution to the camber line.

The complete wing geometry parametrization is completed by the choice of twist,

- local twist angle is parameterized within the functionality in sumo.

III. Transonic Cruise Design

Many different BWB configuration studies have been reported in the literature, e.g. the MOB-Project configuration, the European VELA Projects (3 different layouts), the current NASA X-48 configuration based on Liebeck's design, and many others. We have already worked on a derivative of the MOB configuration, as defined by Ciampa *et al.*[3] for the parametrization of its geometry.

The MOB geometry was made available to us by DLR in the CPACS format developed by DLR.[6] Translators have been developed so that CPACS files can be sent to `sumo` through the wrapping filters,.[31] Note that CPACS supports a wealth of information, such as engine performance data, structural components, etc., of which we use but the exterior geometry. The generality of CPACS enables investigation of eg. aero-elastic design by optimization steps and provides a very general data format for aircraft design, from conceptual design on.

The reference area used for aerodynamic coefficients is $S_{ref} = 1369m^2$ (full span model), with reference length $c_{ref} = 27.4m$, which is the mean aerodynamic chord (MAC).

That BWB geometry has a leading edge sweep angle 64° and low aspect ratio less than 5. This configuration will cause leading-edge suction peaks especially at the tip region. Steady state Euler computations were made from low speed up to transonic speed showing that the maximum Lift-to-drag ratios is about 15 at $M_\infty = 0.65$.[4] This is not competitive with Lift-to-drag ratios $L/D = 21.5$ at $C_L \approx 0.6$. for conventional aircraft.

The challenge for the BWB, as we see it, is transonic cruise at $M_{cr} = 0.8$ where one wants to reach $L/D \geq 22$ for a $C_L \approx 0.3$, i.e. about *136 counts* of total drag, $C_D \approx 0.0136$, i.e., $C_D = C_{D_0} + C_{D_i} \leq 0.0136$. In addition the design must offer acceptable pitching moment and wing-bending moment.

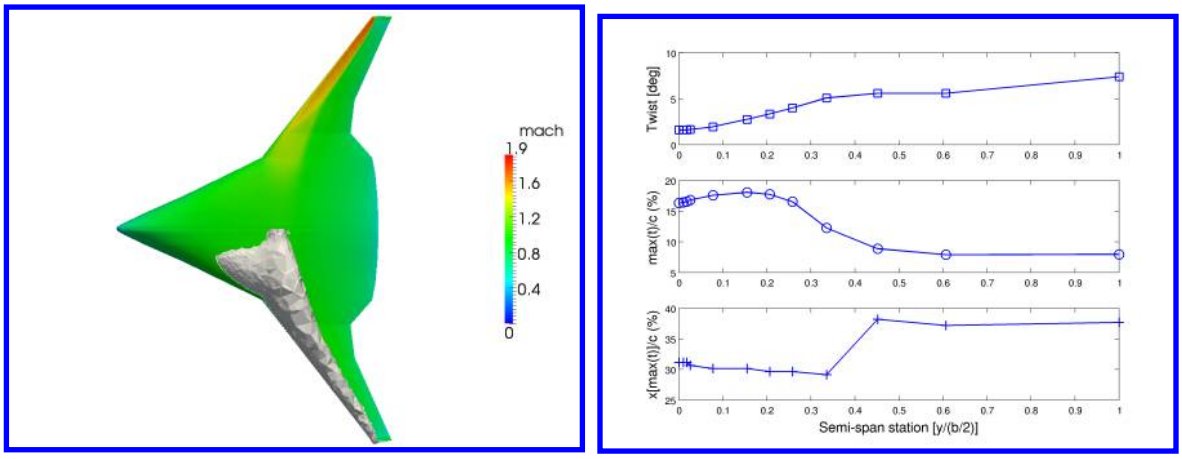

(a) (b)

Figure 6. BWB initial model (a) iso-sonic and isoMach contours at cruise condition $M_{cr} = 0.8$, $C_L = 0.3$; (b) initial platform properties

A. Design Considerations

The initial wing has inviscid drag $C_{D_i} \approx 0.0147$ which exceeds the goal around 50%. Figure 6(a) shows that the local Mach is up to 1.9 at the outer wing, accompanied with a strong shock starting to build-up at the crank. The shock wave is likely to form first from the crank along the outer sections. The very high sweep angle at the inboard wing section makes the outer part of the wing more exposed to the trailing vorticity in

the wake of the inboard wing sections. The sudden reduction of the sweep angle on the outer wing section increases the *effective Mach* locally so the shock forms earlier on that part of the wing.

Note that the initial wing is *washed-in*, namely, the tip wing has more load. The central sections have extremely large thickness-to-chord ratio around 17% while the outer sections are under 10%.

1. *Twist & Camber Design*

We now focus on aerodynamic shape optimization of the BWB, and we adopt the baseline geometry as determined by Ciampa *et al.*,[3] and use it as the starting point for our minimum drag design.

The classical elliptical aerodynamic loading for a conventional aircraft is not the expected optimum for minimum wave drag.[8] Qin *et al.*[8] found a better aerodynamic force distribution to be between the elliptic and triangular spanwise lift distribution. The optimal spanwise lift distribution for best aerodynamic performance at both transonic cruise and low speed climb-out may well be a fine balance of induced drag due to lift and wave drag due to shock wave formation at transonic speeds, perhaps as a combined elliptical/triangular distribution.

A set of eleven profile sections with given thickness and zero camber and twist defines the planar BWB wing. sumo closes the wing tip, creates a triangular surface mesh, and generates a volume grid for Euler simulation using TetGen,[28] as described above.

The starting point for the design is the planar un-cambered and untwisted wing, with the given planform and thickness distribution (Fig 7). The wing surface is then systematically "deformed" on each iteration by

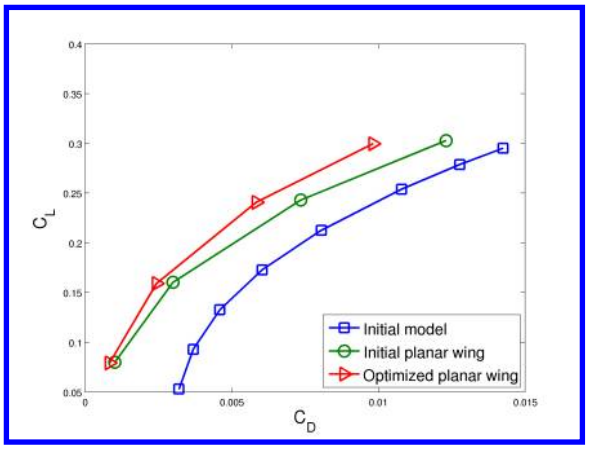

(a) Inviscid drag coefficients comparison at different C_L, cruise $Mach = 0.8$

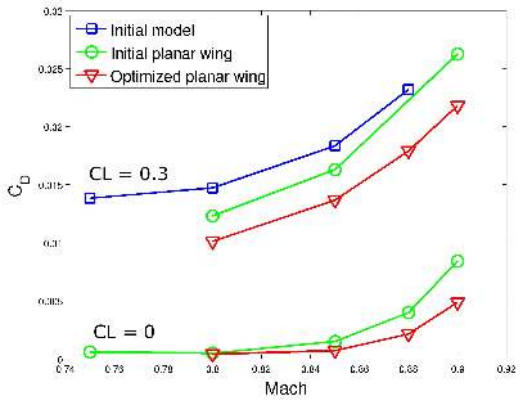

(b) Inviscid drag coefficients for Mach sweep, $C_L = 0$ and $C_L = 0.3$

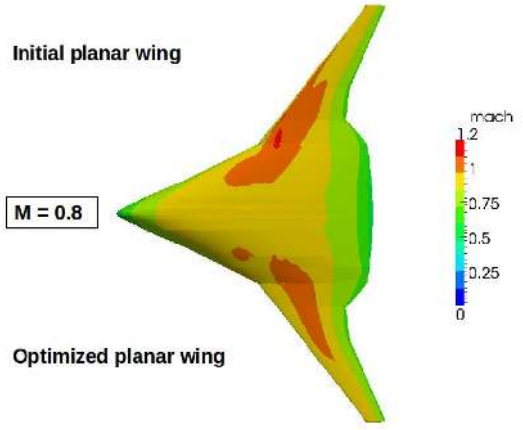

(c) Comparison for Contours of isoMach levles computed in Euler solution on planar BWB surface for $M_{cr} = 0.8$, $C_L = 0$

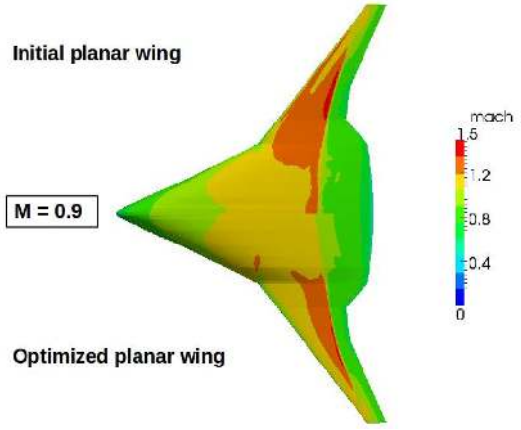

(d) Comparison for Contours of isoMach levles computed in Euler solution on planar BWB surface for $M_{cr} = 0.9$, $C_L = 0$

Figure 7. Some Euler solutions on BWB planar model

varying the design parameters controlling the mean camber line and the twist angle, similar to the procedure described in Meng's thesis[30] but there applied to the inverse design problem

2. Constraints

A satisfactory wing design must demonstrate good performance throughout the flight envelope. The design is therefore subject to high and low speed constraints.

Most transport wings follow the time-honoured guidelines (*e.g.* Kuchemann[23]) for simple isobar pattern at design speed. Further off-design characteristics have to be acceptable. This implies suitable thickness distribution (fuel volume) and local C_L and pitch stability constraints. Camber and twist therefore need to be designed within reasonable planform geometry parameters, without forgetting the aero-elastic behaviour as the design process advances.

Although for minimum drag, spanwise lift distribution is needed, design constraints from structural considerations of e.g. wing bending moment and low speed performance of outer wing may prevent this. Many large aircraft (e.g. A380) use a more triangular spanwise lift loading.

For longitudinal stability, a useful approach for preliminary design is to assume that aircraft is 3-5% MAC stable at low speed and this fixes the CG for high speed. So at high speed $C_m \approx 0$. At low speed that implies need for trim surfaces e.g. *elevons* to be deflected slightly up. Alternatively, fuel and CG management systems come into play as on most civil aircraft currently.

To specify, the constraints applied practically are as follows:

- *thickness taper*, which has been applied by Holmes and Hjelte[24] at KTH in 1953, is also followed as a constraint for the thickness distribution of the three-dimensional flying wing at high speed. It has been shown that a reduction of thickness from the central towards the tips may cause a significant reduction of the velocity increments because of the more three-dimensional nature of the flow. Thickness taper may be combined with a C_L-distribution which increases towards the tip and yet produces fully-swept isobars. This should bring the vortex drag closer to its minimum value.[23]

- *wash-out*, which is always used by wing designers to reduce the lift distribution across the span of the wing. To avoid wing tip stall and aileron ineffectiveness of swept-wing aircraft (stated in Chapter A), the wing is always designed so that the angle of incidence (local twist) is greater at the wing roots and decreases across the span, becoming lowest (always negative) at the wing tip. On aircrafts with highly swept-back wings, the decrease of the local twist angle at the tip would add a nose-up pitching moment, which should be considered to be balanced to get it trimmed.

- *pitching moment* must be sufficient to maintain the stability of the aircraft. A certain stability margin has to be achieved. In cruise, the aircraft should also be trimmed: so that the lift is not lost to control surface deflections. In this condition the trim drag is also small, with L/D the best. At low speed, the neutral point would shift forward. With a too small *static margin* (SM), it might be unstable at low speed and hard to control by the pilot.

- *bending moment*, is always considered as the first step towards aero-structural design. The wing is likely to bend towards the center of gravity (CG). It might cause aeroelastic problems when the aerodynamic forces couples with the structure's natural mode of vibration to produce rapid periodic motion, such as flutter or aileron reversal. A practical factor to look into is the local C_L (C_{LL}) on the wing. For this BWB case the $C_{LL,max}$ should not exceed 0.65, as indicated by Nangia *et al.*[25]

Besides, the cabin box in the central body has to fit into the geometry; and the cruise angle of attack (AoA) should be such to keep the cabin floor level.

IV. Results and Discussion

A. First Step Optimized Design – Start with planar wing

We start with the planar wing, all twists and cambers are zero, only the thickness of the airfoils is kept. Figure 9(a) shows the planar BWB geometry created in sumo and used as the start of the optimization procedure. The airfoil's thickness distributions are free to change from the tip to the inboard part close to central. Figure 7(c) shows that at cruise condition $M_{cr} = 0.8$ a mild shock forms first at the outer part of

the wing at zero angle of attack (*i.e.* zero lift). The flow reaches up to a local Mach number of $M = 1.2$ in the red region of Fig. 7(c), and this is not a good sign because if the planar wing already has supersonic flow, adding twist and camber might make it worse, and finding an acceptable wave drag will be very difficult. The wing thickness to chord ratio may as well be too high for efficient $M = 0.8$ cruise. The optimized planar wing reduces the wave drag coefficient from *4.8 counts* to *3.3 counts*, around 31% reduction.

The wave drag at $M = 0.8$ computed by Edge at zero lift is only a few *counts*). Thus, the induced drag C_{D_i} is comparably large especially at higher C_L, due to the appearance of the shock, and it becomes stronger with increasing $Mach$ and C_L (Fig. 7(b)). The optimal thickness distribution for the planar wing serves to reduce the drag at the design point, *ie*, cruise condition $M = 0.8$ and $C_L = 0.3$, as well as for higher Mach numbers.

Figure 8 shows that at design cruise condition the shock is significantly weakened. The improved thickness

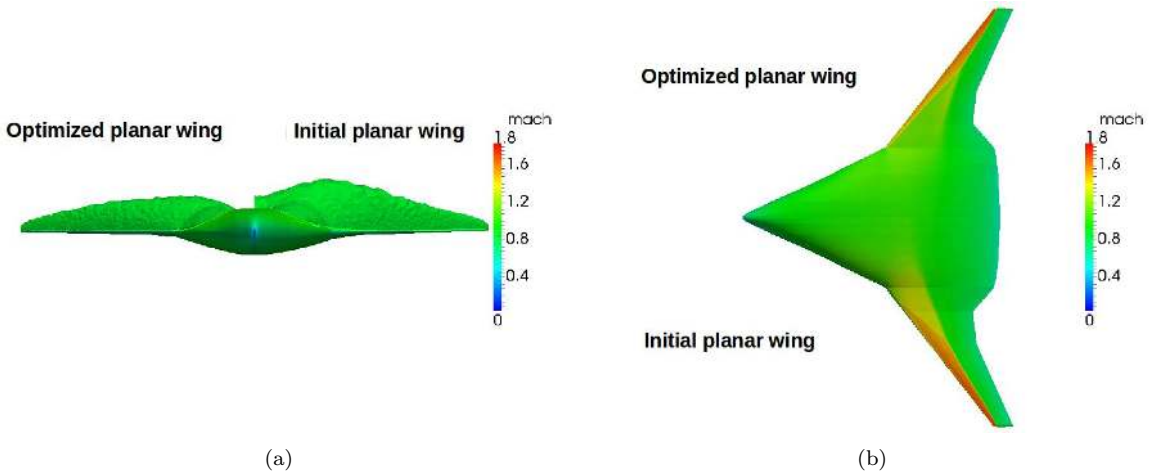

(a) (b)

Figure 8. BWB planar model: initial planar model v.s. the optimized one, at cruise condition $M_{cr} = 0.8$; $C_L = 0.3$ (a) iso-sonic contours; (b) isoMach contours

distribution reduces the shock dramatically especially from the crank down to the tip. This phenomenon corresponds to Figure 9 the thickness reduction from a bit inboard of the crank ($y_{station} = 17.5m$), and a huge reduction at the crank ($y_{station} = 13m$). The station before the crank also has an influence on the flow at the crank and down to the tip, since the high-swept central part makes the outer part more exposed to the vorticity in its shed wake.

B. Second Step Optimized Design - adding the camber and twisting the wing

The cambers and twists are always coupled, the goal is to further reduce the drag while providing enough lift. The Angle of Attack (AoA) will be reduced as well. The cruise AoA for civil airliner is supposed to be small, around 3° is acceptable. The drag is further reduced, while the pitching moment and bending moment are considered at the same time. Due to the configuration type which has a blended wing body at central, the centre of gravity is a bit aft compared with conventional aircraft, located at 35% MAC. It is calculated that the BWB is trimmed ($C_m \approx 0$) for its 4^{th} step optimized model, with 45% inviscid C_D reduction from the initial model. It is obtained by first varying camber and then varying twist on the optimized planar wing (2^{th} step optimized design in 11). Figure 10 shows the camber lines and the local twists for this model. The outer wing has negative twist that releases loading at the tip, consistent with modern aircraft design rule that the wing is favourable to have *washout*. Note that the tip twist is quite large to release loads. The optimal design is constrained by the selected constraints, to be expected.

C. Optimized Design Discussion

There are two main steps to iterate to a better design, as stated above. If we look closely at Figure 11, we can see that we start with the initial wing, or 0^{th} step, then the inviscid drag is reduced first by removing all the twists and cambers, when the configuration becomes a planar wing, or the 1^{st} optimized design step. We have to say the initial wing is a "bad" design, it makes its behaviour worse by adding the cambers and the

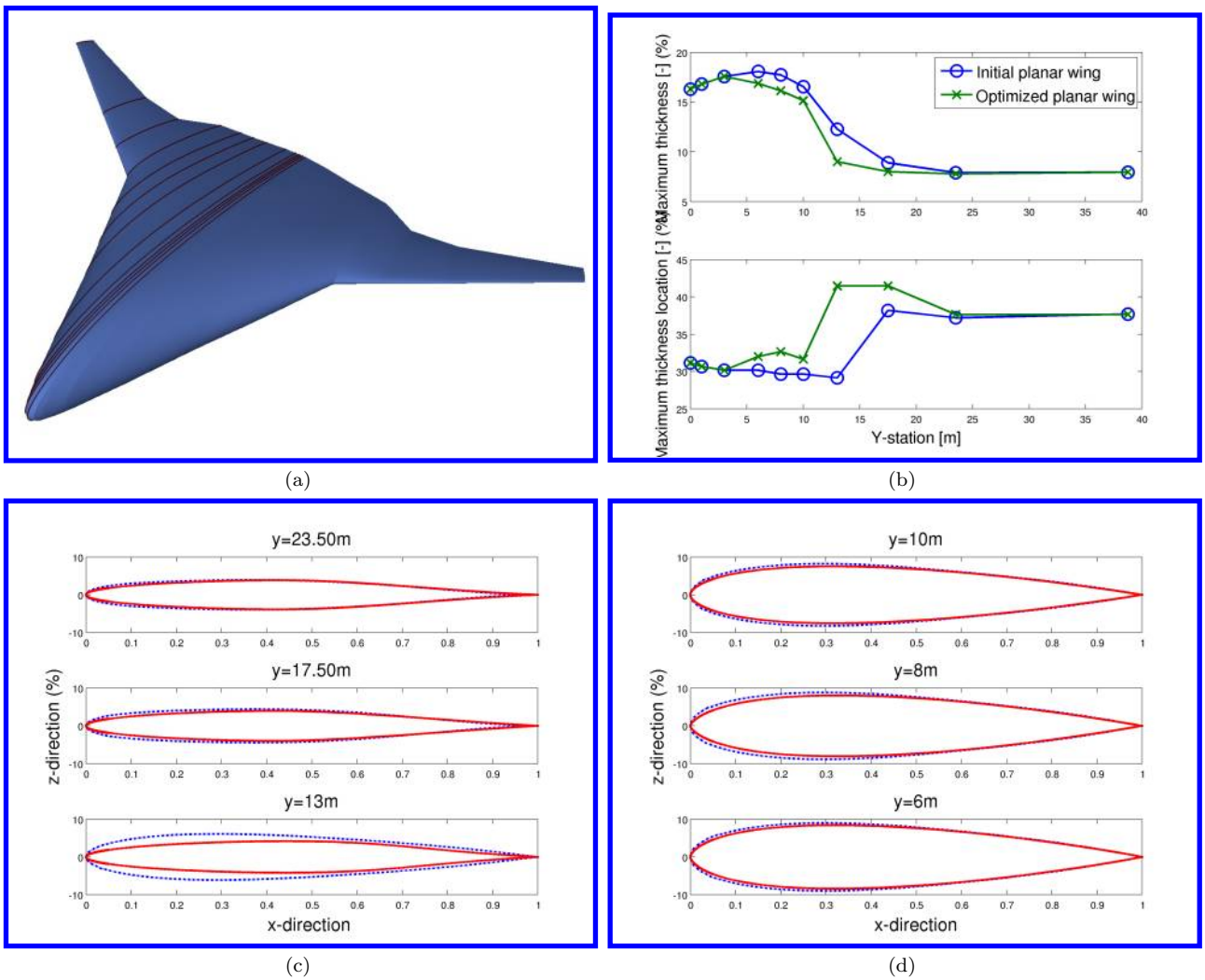

Figure 9. Thickness distribution design on the planar BWB geometry. (a) The planar BWB geometry with given planform and airfoil-section thickness - the starting design model; (b) Comparison of the thickness distribution between the initial planar wing and the optimized planar wing; (c) & (d) Comparison of the airfoils between the initial planar wing and the optimized planar wing, at different spanwise stations, red: initial airfoil thickness; blue: optimized airfoil thickness

twists. The re-designed thickness distribution makes the inviscid drag further reduced by 20% from about 0.0125 to 0.01. The further reduction is made by varying the twists and the cambers with fixed thickness distribution. There are two independent approaches to take. One is to follow the red arrow in Figure 11 by first varying the camber (the 3^{rd} optimized design step) and then varying the twist (the 4^{th} optimized design step), from the optimized planar wing (the 2^{nd} optimized design step), as stated in Section B. We ended up with the 4^{th} step optimized design, with the inviscid drag reduced further by around 19% from around 0.01 to 0.0081, and the aircraft trimmed at this stage as well (Fig 13(a)). The other approach is to couple the camber and twist variation together, following the blue arrow in Figure 11, by varying the camber and twist at the same time, from the optimized planar wing (the 2^{nd} optimized design step). The drag is further reduced to a even lower value by 25% from the 2^{nd} step optimized design, while the trim condition can not be maintained. This is still quite useful if we further consider the planform into the optimization loop. To remedy this, in general the neutral point should be shifted a bit forward to obtain good flying qualities, thus the wing part (*i.e.*, the outer wing) can be shifted a bit forward to move the neutral point, while the CG position is almost unchanged. Struber[26] did the similar optimization by varying the chord length (fixed sweep angles) in addition to the airfoils shape and local twist, resulting a configuration with the central part quite aft and outer wing part shifted quite forward. The author also obtained the trim condition ($C_m \approx 0$)

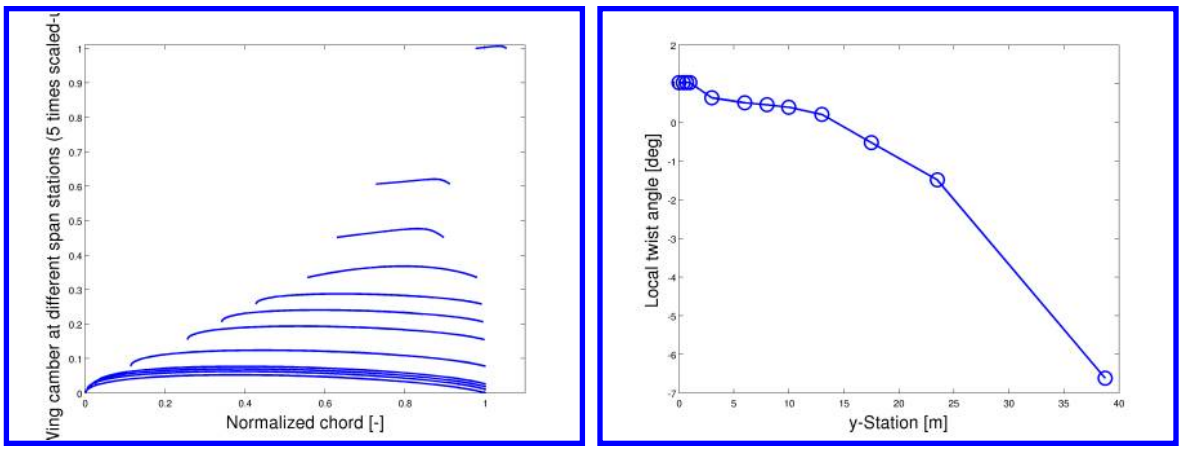

(a) (b)

Figure 10. BWB optimized design, (a) camber lines for different $y_{station}$ from root to tip, normalized by root chord; (b) local twist angle

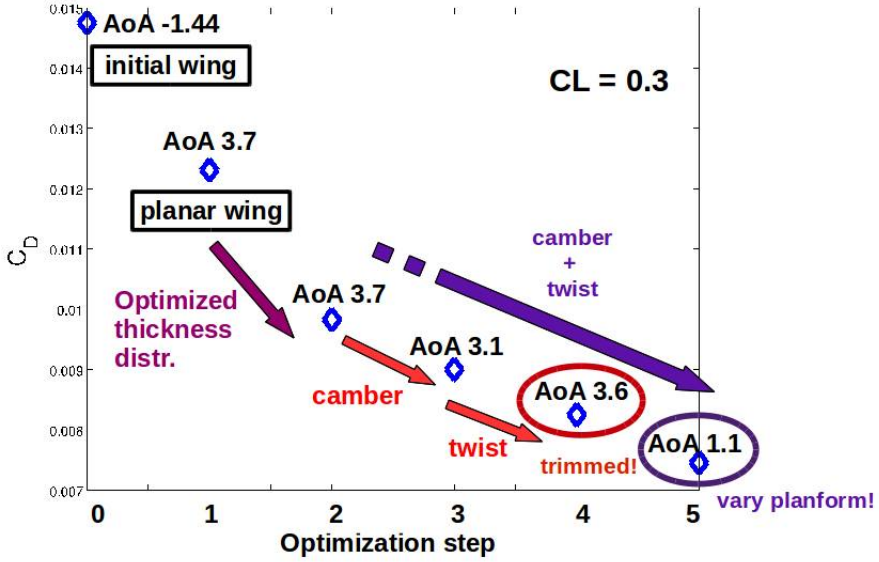

Figure 11. BWB optimal design, optimization main steps for C_D

if the outer part of wing shifted 3 meters, or 10% MAC forward, and it is called the 5^{th} step of optimized design (Fig. 13(b)).

The initial wing has a local Mach up to 1.9, and forms a strong shock early from the crank down to the tip. The 4^{th} step optimized wing reduces the shock quite a lot, while the 5^{th} step optimized wing almost eliminates the shock at the crank and it only has a mild shock further down to the tip. Note that the 4^{th} step optimized design almost completely remove the shock at the tip, while pushing it a bit inboard.

Now we talk more about why the optimized model has less drag, or, better design. Figure 14(b) and 14(c) show the span loads and local lift coefficient C_{LL} for each iteration, recalling the Fig. 11. The 0^{st} step, or the initial MOB, the root is not carrying sufficient loads, while the tip is over loaded. This design is dangerous that the tip is quite likely to stall first, as we can see the strong shock existing at the wing tip in 6(a). Also the loss of effectiveness of moving devices mounted at the tip is also dangerous, especially for the flying wing, whose 3 DOFs moments are all controlled by the quite swept-afterward wing tip devices. The optimal MOB has small loads at the tip, while almost the constant loads at the central part until the crank.

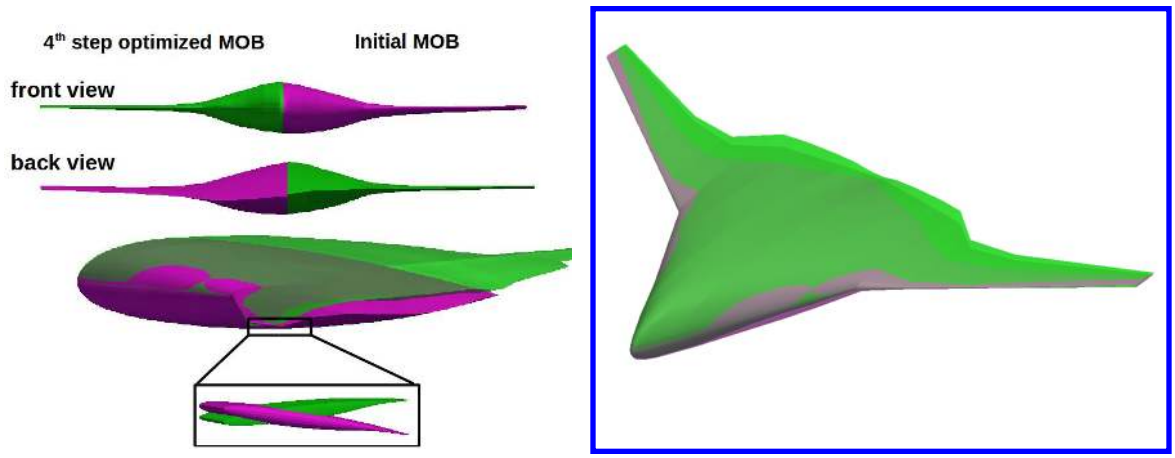

(a) (b)

Figure 12. Geometry comparison between the initial MOB (magenta) and the 4^{th} step optimized MOB (green)

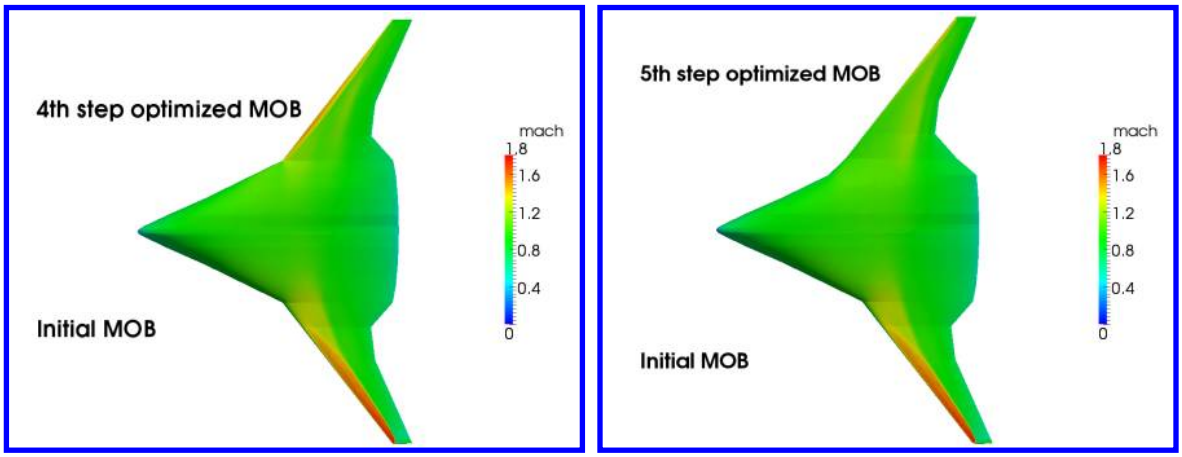

(a) BWB optimal design, optimization main steps for C_D (b) Comparison of the isoMach contours for the initial wing and the 4^{th} step optimized design

Figure 13. Euler predictions on optimized design of BWB for different steps, for $C_L = 0.3$ at $M = 0.8$

After the crank, the span-load distribution is more like a triangular. This is consistent with what Qin[8] has stated. The local pressure distribution (C_p) is refined to avoid leading edge suction (significant C_p peaks) and strong shocks (pressure jump) while improving the drag. The pressure distribution is overall refined, especially near the crank and the outer part, which are quite critical for the drag. Note that the flow at central part also influences the outer region of the wing. The mathematical optimization algorithm is highly coupled with aerodynamics in this design. A simply reduction of drag in number does not necessarily lead to a good design.

An Reynolds-Averaged Navier-Stoke (RANS) computation on the planar wing has been carried out at the beginning. The viscous drag is almost 0.0054, so we have the total drag coefficient at designed lift $C_L = 0.3$:

$$C_{D,total} = C_{D,pressure} + C_{D,friction} = 0.00807 + 0.0054 = 0.0135 \quad (2)$$

Thus, we have the L/D at designed cruise point $L/D = 22.3 > 21$ for the 4^{th} step optimized design, the design goal is met.

D. Design Analysis & Remarks

The work is half-done if we only consider "one-point solution". Usually we would like to have an aircraft with best performance along its flight, not only at one single point. Figure 7(b) already shows that the

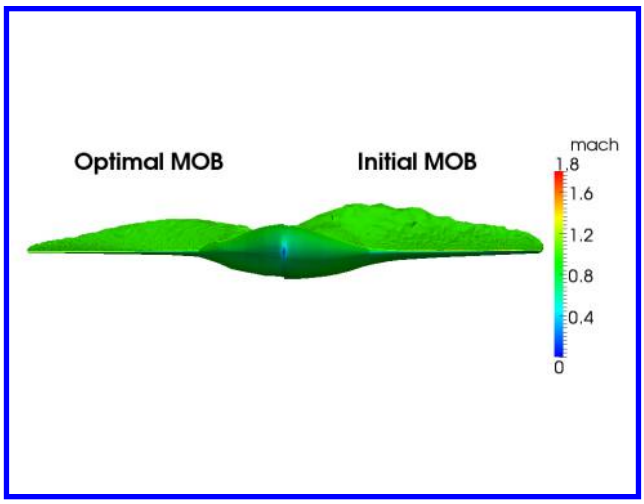

(a) iso-sonic contours at cruise condition

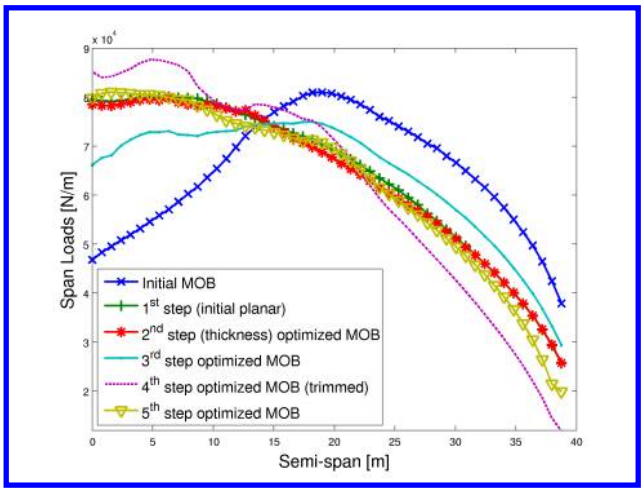

(b) Span Loads

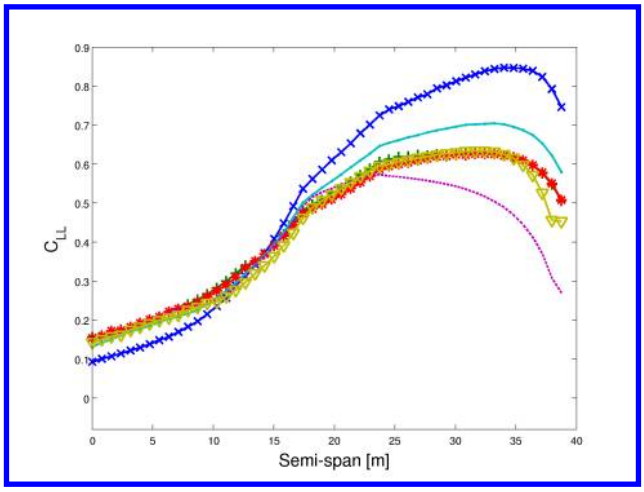

(c) Local C_L

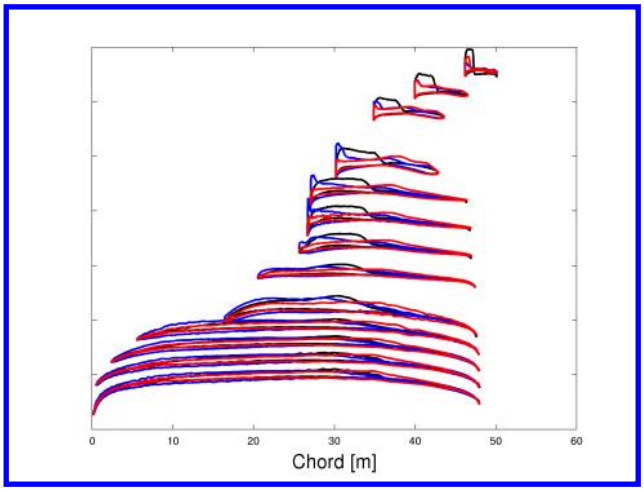

(d) Local pressure distribution C_p, quantity demonstration; black line: initial wing; blue line: 4^{th} step optimized model; red line: 5^{th} step optimized model

Figure 14. Comparison between the initial wing and the optimized design in some aspects, computed by Euler Edge, for $C_L = 0.3$ at $M = 0.8$

design follows a promising trend as Mach number increases. Now we concentrate a bit on flying for varied C_L, or AoA. Figure 15 shows two different measuring criteria, drag polar and L/D curve. Both of them indicate that both the 4^{th} and the 5^{th} step optimized designs meet the requirements, not only for the cruise point at $C_L = 0.3$.

Figure 16 shows that the pressure coefficient (CP) contour comparisons on the upper surface between the 4^{th} and 5^{th} step optimized designs and the initial one. For both optimized designs the magnitude of the negative pressure has been weakened, while the area of the low pressure region is not reduced, resulting a "milder" shock compared with the initial model. Figure 17 and Figure 18 show the comparisons for the airfoils and sectional CP of the three models (initial model: marked by black; the 4^{th} step optimized model: marked by blue; the 5^{th} step optimized model: marked by red) at four spanwise stations. The stations are labeled in Fig. 16(a).

For the inboard stations ($\eta = 0, 0.15, 0.33$), the optimized models are more twisted than the initial one, while the airfoils from 5^{th} step optimized model are a bit more cambered than the 4^{th} step optimized one. The CP is generally refined at the central sections. At the crank, where the initial model has a significant pressure jump (shock forms), the 5^{th} step optimized design (red) (Fig. 18(b) for $\eta = 0.33$) almost gets rid of the sharp pressure jump, thus the shock is reduced quite a lot, if we recall Fig. 16(b) and Fig. 13(b), where only a mild shock exists at the crank sitting at around 50% downstream.

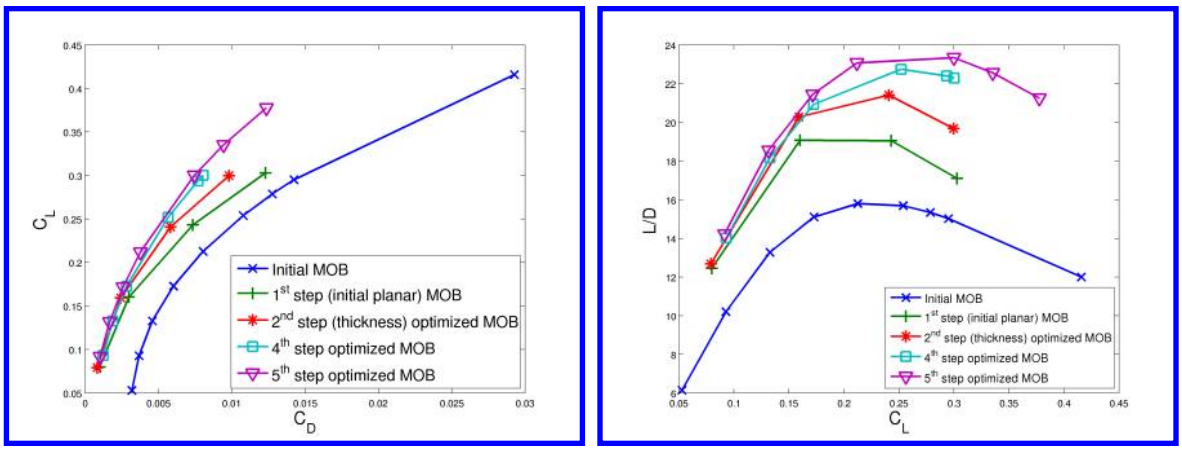

(a) Drag polar (b) L/D

Figure 15. Euler predictions on BWB optimized design and its iterations, at $M = 0.8$ for a range of C_L (or AoA)

The 4^{th} step optimized design at crank is not as good as the 5^{th} step optimized one. It brings a negative pressure peak at the leading edge, which we should try to avoid. On the other hand, at the wing tip, or $\eta = 0.98$, the 4^{th} step optimized design completely removes the pressure jump, that almost eliminates the shock at the wing tip. It results a safer design at the wing tip, compared with the 5^{th} step optimized model, which weakens the pressure jump a bit but still has shocks.

Future optimization should start from those two designs, by keep their pros and refining their cons. From the solution of 5^{th} step optimized design we are aware that the next optimization step should introduce the planform as design parameters as well.

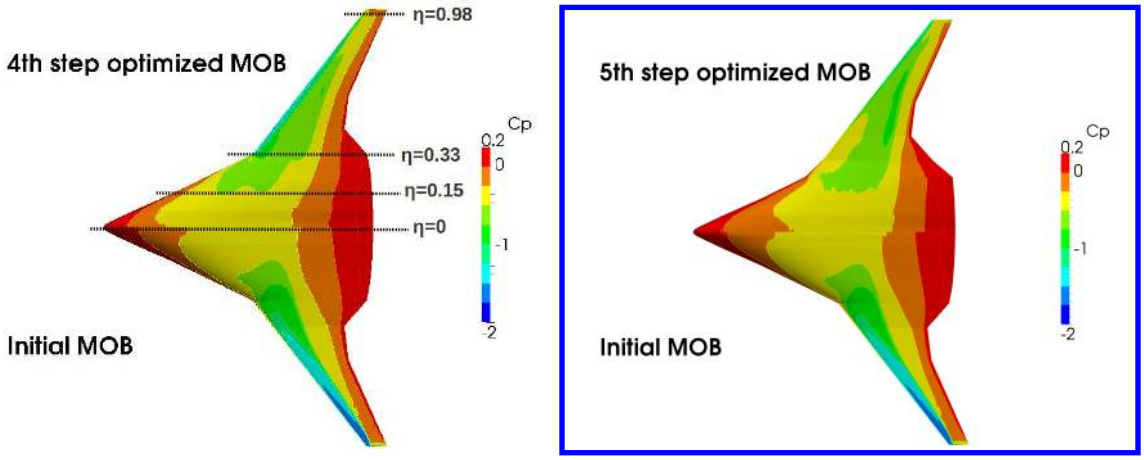

(a) (b)

Figure 16. CP contours Euler solutions, upper surface

To make sure that the flying wing has sufficient flying handling qualities, we would like to find out the location of its *aerodynamic center*, the point about which the pitching moment is independent of the lift. The x_{ac} travels aft when the airspeed increases. Figure 19 shows how the aerodynamic center location shifts *w.r.t.* the CG position with Mach number for the 4^{th} optimized design. This is also called *static margin*, that measures the static stability of the airplane with respect to the small incident disturbances. It can be seen that at cruise Mach 0.8, the SM is a bit below 4%, which is a bit small for conventional civil transports. It is slightly stable (or neutral stable) down to Mach number 0.5. For modern piloted aircrafts, the stability can be maintained by pilot control or fly-by-wire system, which is not so critical as other aspects in aircraft design.[29]

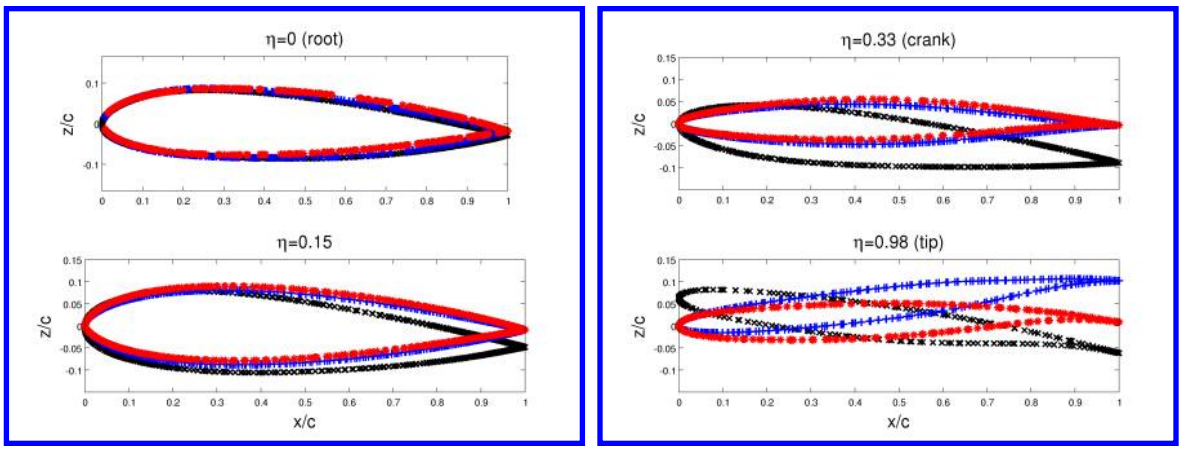

(a) (b)

Figure 17. BWB geometry comparison, four spanwise stations, black: initial MOB; blue: the 4^{th} step optimized MOB; red: the 5^{th} step optimized MOB

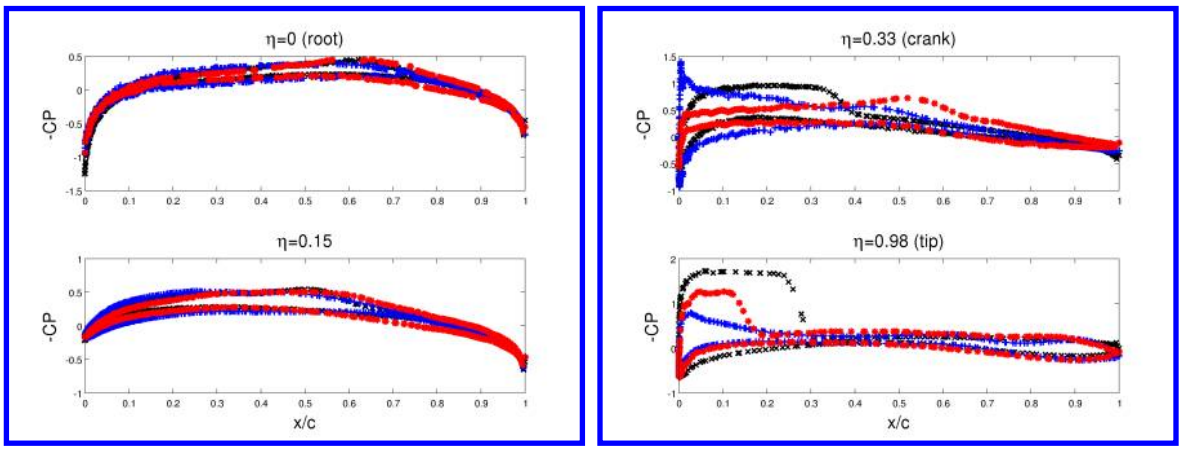

(a) (b)

Figure 18. BWB CP comparison, four stations,black: initial MOB; blue: the 4^{th} step optimized MOB; red: the 5^{th} step optimized MOB

E. Thoughts of Future Work

The optimization work can be further proceeded to get a better design. The camber line shape can probably be improved. For example, reflex camber at the inner sections increases the effective leading edge suction where it is relatively lower. Alternatively, allowing the tip section to reflex might be a good way to trim and balance a clean wing combined with washout at the tips.

The considerations to change the planform would be first to change the leading edge position, or shift the wing fore (or aft), just as the 5^{th} step optimized design, which shifts the wing part forward resulting a shift of the neutral point while the total lift is maintained. Next we maybe would like to consider to fix the sweep angle and change the chord length, *i.e.* we change the taper ratio by stretching or shrinking the chord. Changing the planform would add more design degrees of freedom, it is important to keep it simple at first and make it easy to implement.

V. Conclusions

This paper represents the optimization work for the transonic flying wing: the blended wing body transport. The authors describe an efficient and robust technique to do the geometry parametrization, with Euler

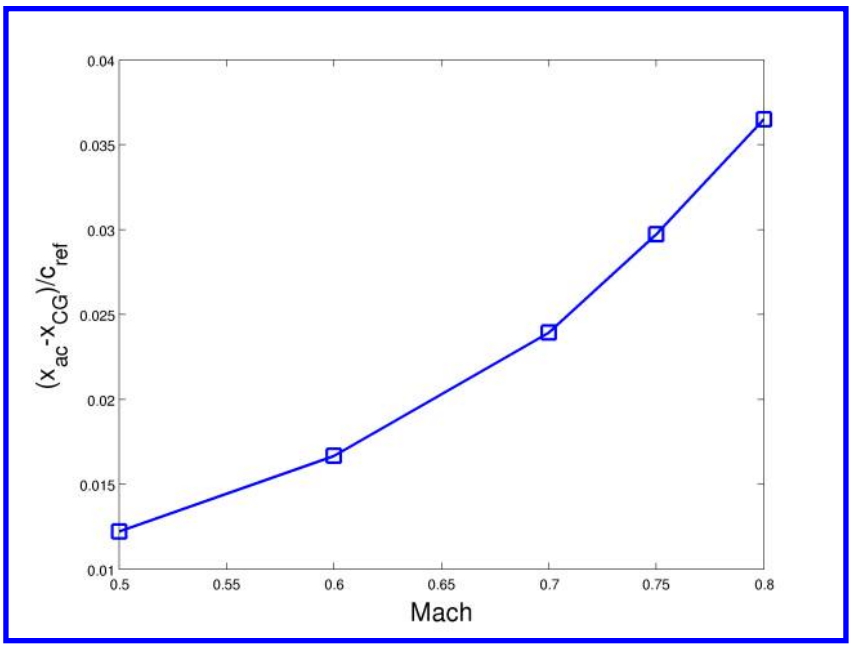

Figure 19. Computed aerodynamic center location x_{ac} relative to CG by Euler predictions on BWB 4^{th} step optimized design

mesh re-generated every iteration. The work is then straight forward and easy to understand. Engineer must be involved in the design loop, to guide the direction of the optimization work. The optimized results show that it is converged towards the design goal. With the fixed planform, the inviscid drag is reduced by about 45% at the designed lift. The aircraft is trimmed at this point, with static margin slightly positive. The wing root is highly loaded, and the tip load is reduced quite a lot compared with the initial design. However, it introduces suctions at some span wise stations of the leading edge, which ought to be avoided. An attempt at further improvement is made, by not only parameterizing the wing profile shape and local twist, but also the planform. It shows that the results can be improved by introducing more design parameters and more strict constraints.

Acknowledgment

This work was supported by the Swedish National Infrastructure for Computing via the PDC Parallel Computer Center at KTH.

References

[1] http://www.albentley-drawings.com/main.htm. (accessed 20 August 2012).

[2] http://www.nasa.gov/centers/langley/news/factsheets/FS-2003-11-81-LaRC.html. (accessed 20 August 2012).

[3] Ciampa P. D., Zill T., Pfeiffer T. and Nagel B., "A Functional Shape Parametrization Approach for Preliminary Optimization of Unconventional Aircraft", 3rd CEAS Air&Space Conference, Venice, Italy, 2011.

[4] Rizzi A.,Zhang M., Nagel B., Boehnke, D. and Saquet P., "Towards a Unified Framework using CPACS for Geometry Management in Aircraft Design", 50th AIAA Conference, Nashville, TN, 2012.

[5] Kchemann D. *The Aerodynamic Design of Aircraft: A detailed introduction to the current aerodynamic knowledge and practical guide to the solution of aircraft design problems*, 1st edition 1978. ISBN 0-08-020514-3.

[6] Boehnke, D.,"Common Parametric Aircraft Configuration Schema CPACS", v1.7, available at: http://software.dlr.de/p/cpacs/home/(2011).

[7] Eller D., "Larosterna Engineering Dynamics Lab, Aircraft Modeling and Mesh Generation", available at: http://www.larosterna.com/sumo.html (accessed 01 June 2011).

[8] Qin N., Vavalle V., Le Moigne A., Laban M., Hackett K., Weinerfelt P., "Aerodynamic considerations of blended wing body aircraft", Progress in Aerospace Sciences 40 (2004) 321-343.

[9] Eliasson, P., "Edge, a Navier-Stokes solver for unstructured grids", in Proc. Finite Volumes for Complex Applications III, ISBN 1 9039 9634 1, pp.527-534, 2002.

[10] Amoignon, O. and Berggren, M., "Discrete adjoint-based shape optimization for an edge-based finite-volume solver", In K. J. Bathe, editor, Computational Fluid and Solid Mechanics 2003, pages 2190–2193. Elsevier Science Ltd, 2003.

[11] Amoignon, O. and Berggren, M., "Adjoint of a median-dual finite-volume scheme: Application to transonic aerodynamic shape optimization", Department of Information Technology, Uppsala University, Technical Report 2006-013, 2006.

[12] Amoignon, O., *AESOP: a program for aerodynamic shape optimization, Optimization and Engineering*, Springer, Volume 11, Number 4, December 2010 , pp. 555- 581(27)

[13] Nocedal, J. and Wright, S. J., *Numerical Optimization*, Springer, 2006. ISBN 0-387-30303-0. http://www.ece.northwestern.edu/ nocedal/book/num-opt.html.

[14] Qin, N., "Spanwise Lift Distribution for Blended Wing Body Aircraft", J. Aircraft, Vol.42, No.2, March-April 2005.

[15] Lamar, J., "A Vortex Lattice Method for the Mean Camber Shapes of Trimmed Non-Coplanar Planforms with Minimum Vortex Drag", NASA TN-D-8090, June 1976.

[16] Grant, F., "The Proper Combination of Lift Loadings for Least Drag on a Supersonic Wing", NACA Rep. 1275, 1955.

[17] M. A. Potsdam, M. A. Page, and R. H. Liebeck, "Blended Wing Body Analysis and Design", AIAA-Paper 1997-2317, June 1997.

[18] Griva, I., Nash, S. G., Sofer, A., *Linear and Nonlinear Optimization*, 2nd edition 2008. ISBN 978-0-898716-61-0.

[19] Venkataraman P, "Low Speed Multipoint Airfoil Design", Rechester Institute of Technology, 16th Applied Aerodynamic Conference, Albuquerque, New Mexico, 1998.

[20] Morris, A., "MOB: A European Distributed Multi-Disciplinary Design and Optimization Project", Proceedings of 9th AIAA Symposium on Multidisciplinary Analysis and Optimization, AIAA Paper 2002-5444, Atlanta, Georgia, 4-6, September 2002.

[21] Nangia, R.K., Boelens, O.J., Tormanlm, M. "A Tale of Two UCAV Wing Designs", AIAA 2010-4397, 2010.

[22] Tomac, M., Rizzi, A., Nangia, R.K., Mendenhall, M.R., Perkins, Jr., S. C., "Engineering Methods Applied to a UCAV Configuration - Some Aerodynamic Design Considerations",

[23] Kuchemann, D. F.R.S., *The Aerodynamic Design of Aircraft*, 1st edition 1978. ISBN 0-08-020514-3.

[24] Holme, O., Hjelte, F. "One the Calculation of the Pressure Distribution on Three-Dimensional Wing at Zero Incidence in Incompressible Flow"

[25] Nangia, R. K., Palmer, M. E., and Doe, R. H.,"Aerodynamic Design Studies of Conventional & Unconventional Wings with Winglets", AIAA 2000-3400, 2000.

[26] Struber, H., Hepperle, M., "Aerodynamic Optimisation of a Flying. Wing Transport Aircraft", Notes on Numerical Fluid Mechanics and Multidisciplinary Design, 2006, Volume 92/2006, 69-76,

[27] Whitford, R., *Design for Air Combat*, ISBN 0 7106 0426 2.

[28] Si, H., "TetGen: A Quality Tetrahedral Mesh Generator and a 3D Delaunay Triangulator", available at: http://tetgen.berlios.de/ (accessed 28 June 2012).

[29] Raymer, D. P., *et al.*, "Advanced Technology Subsonic Transport Study: N+3 Technologies and Design Concepts", NASA/TM-2011-217130, November 2011.

[30] Meng, P., "Aerodynamic Shape Optimization for the SACCON UCAV", MSc Thesis, KTH, Stockholm, 20012.

[31] Nagel, B., Bhnke, D., Gollnick, V., Schmollgruber, P., Rizzi, A., La Rocca, G., Alonso, J. J., "Communication in Aircraft Design: Can we establish a Common Language?", 28th International Congress of the Aeronautical Sciences, ICAS 2012.